A CORRECTION TO MCIP CALCULATION OF VERTICAL CONTRAVARIANT VELOCITY OF NON-HYDROSTATIC MM5 IN MCIP AND ITS IMPACT ON AIR QUALITY SIMULATION

Fuquan Yang*, Jack Chen, Weimin Jiang, Helmut Roth, Steven C. Smyth,
Institute for Chemical Process and Environment Technology, National Research Council of Canada, Ottawa, Ontario, Canada

1. INTRODUCTION

The contravariant vertical velocity used in the Community Multi-scale Air Quality (CMAQ) Model is calculated by the Meteorology-Chemistry Interface Processor (MCIP). It is a key parameter in controlling vertical advection and describing the static stability of atmosphere. Large errors in the vertical wind can significantly deteriorate the consistency between the air density and wind fields. Such consistency is a fundamental requirement to ensure mass consistency in air quality modeling studies (Byun, 1999).

Recently, we found an error in MCIP (version 3.2 and its earlier versions) in the computation of the contravariant vertical wind velocity. Instead of using the surface reference state pressure, the total surface pressure from the first time period processed by MCIP was mistakenly used in the calculation of contravariant vertical velocity.

The error led to unphysical contravariant vertical wind fields, caused exaggerated perception of air mass inconsistency within the non-hydrostatic MM5 meteorological model outputs, and affected the advection scheme analysis. After the error was reported, it was subsequently corrected in the current release of MCIP version 3.3.

This paper presents a detailed analysis of the error and the correction. It also shows the impacts of the correction on the extent of CMAQ mass consistency adjustment and advected tracer concentration.

2. CORRECTION OF THE CONTRAVARIANT VERTICAL VELOCITY ERROR

**Corresponding author:* Fuquan Yang, National Research Council of Canada, Room 233, M2,1200 Montreal Road, Ottawa, Ontario, Canada K1A 0R6; e-mail: Fuquan.Yang@nrc-cnrc.gc.ca

2.1 Calculation of the contravariant vertical velocity in MCIP

In MCIP, the contravariant vertical wind velocity should be calculated as (Byun, 1999):

$$\dot{\xi} = \left[\frac{\sigma_{p0}}{p^*} \frac{\partial p_0^*}{\partial \hat{x}^1} \right] (mu) + \left[\frac{\sigma_{p0}}{p^*} \frac{\partial p_0^*}{\partial \hat{x}^2} \right] (mv) + \frac{\rho_0 g}{p^*} w \qquad (1)$$

where, $\dot{\xi}$ is the contravariant vertical wind velocity, mu and mv are map scaled wind velocities along the $\hat{x}^1$ and $\hat{x}^2$ direction, w is the normal vertical wind velocity component from non-hydrostatic MM5, σ_{p0} is the sigma value, ρ_0 is the reference state air density, g is gravitational acceleration constant, and p^* is the difference between the reference state surface pressure (p_{s0}) and the model top pressure (p_t) , i.e.,

$$p^* = p_{s0} - p_t \qquad (2)$$

The reference state surface pressure can be calculated from:

$$p_{s0} = p_{00} \exp\left(\sqrt{\left(\frac{T_{00}}{A}\right)^2 - \frac{2gH}{RA}} - \left(\frac{T_{00}}{A}\right) \right) \qquad (3)$$

where R is the gas constant for dry air , H is the terrain height, P_{00} is the sea level pressure (100,000Pa), T_{00} is the temperature at P_{00} (290 K), and A is the temperature lapse rate (50K), representing the temperature difference between P_{00} and P_{00}/e = 36788 Pa. The model reference state does not change with time in the simulation.

2.2 Error in the calculation of the contravariant vertical velocity in previous MCIP versions

In the previous MCIP versions (version 3.2 and earlier), the p^* in equation (1) was incorrectly calculated as the difference between the total surface pressure from the first time period processed by MCIP (p_s) and the pressure at the model top, i.e.,

$$p^*_{incorrect} = p_s - p_t \, . \tag{4}$$

The total surface pressure, p_s , in Eq. (4) is calculated by adding the perturbation pressure p' from the first time period processed by MCIP to the surface reference state pressure, i.e.,

$$p_s = p_{s0} + p' \tag{5}$$

where $p' << p_{s0}$. From Eqs. (4) and (5), we can get:

$$p^*_{incorrect} = p_{s0} + p' - p_t \, . \tag{6}$$

From Eqs.(2) and (6), it can be easily seen that the perturbation pressure from the first time period processed by MCIP was introduced into the calculation of the incorrect p^* in Eq. (4). The incorrect p^* was then used to calculate the contravaraint vertical velocity in Eq. (1).

Note that this error exists only when the non-hydrostatic MM5 results are processed by MCIP and the vertical contravariant wind velocity generated by MCIP is used in CMAQ. It does not exist for the calculation of contravariant vertical velocity with hydrostatic MM5 and has no impact on CMAQ simulations that use the Yamartino scheme where the contravariant vertical velocity is recalculated in CMAQ.

2.3 Mathematical differences between the incorrect and the correct contravariant vertical velocities

Mathematically, the difference between the incorrect and the correct contravariant vertical wind velocities can be expressed as:

$$\dot{\xi}_{incorrect} - \dot{\xi} = \left[\frac{\sigma_{p0}}{p^*_{incorrect}} \frac{\partial p^*_{incorrect}}{\partial \hat{x}^1} - \frac{\sigma_{p0}}{p^*} \frac{\partial p^*}{\partial \hat{x}^1} \right] (mu) + \left[\frac{\sigma_{p0}}{p^*_{incorrect}} \frac{\partial p^*_{incorrect}}{\partial \hat{x}^2} - \frac{\sigma_{p0}}{p^*} \frac{\partial p^*}{\partial \hat{x}^2} \right] (mv) + \left(\frac{\rho_0 g}{p^*_{incorrect}} - \frac{\rho_0 g}{p^*} \right) w \tag{7}$$

where $\dot{\xi}_{incorrect}$ and $\dot{\xi}$ are the contravariant vertical velocities calculated by the previous (v3.2 and older) and the current (v3.3) MCIP versions, respectively.

The three terms on the right-hand side can be approximated as:

$$\left[\frac{\sigma_{p0}}{p^*_{incorrect}} \frac{\partial p^*_{incorrect}}{\partial \hat{x}^1} - \frac{\sigma_{p0}}{p^*} \frac{\partial p^*}{\partial \hat{x}^1} \right] (mu) \cong \frac{\sigma_{p0}}{p^*} \frac{\partial p'}{\partial \hat{x}^1} (mu) \tag{8}$$

$$\left[\frac{\sigma_{p0}}{p^*_{incorrect}} \frac{\partial p^*_{incorrect}}{\partial \hat{x}^2} - \frac{\sigma_{p0}}{p^*} \frac{\partial p^*}{\partial \hat{x}^2} \right] (mv) \cong \frac{\sigma_{p0}}{p^*} \frac{\partial p'}{\partial \hat{x}^2} (mv) \tag{9}$$

$$\left(\frac{\rho_0 g}{p^*_{incorrect}} - \frac{\rho_0 g}{p^*} \right) w \cong 0 \tag{10}$$

The derivation processes for the above equations are not given here for brevity.

From Eqs. (8), (9) and (10), it can be seen that the difference of the contravariant vertical wind velocity at a specified time is largely produced by the contravariant horizontal wind velocity (mu, mv) at that time and the gradient of perturbation pressure ($\frac{\partial p'}{\partial \hat{x}^1}$ and $\frac{\partial p'}{\partial \hat{x}^2}$) from the first time period processed by MCIP.

The perturbation pressure from the first time period processed by MCIP is kept to be constant in the incorrect MCIP run and is used to calculate the contravariant vertical velocity. Even for the same non-hydrostatic MM5 output, the errors of the contravariant vertical velocity generated by different runs of the incorrect MCIP are different if the runs start from different times.

Since the magnitude of formula Eq. (10) approximates zero, the sign of the left hand side of Eq. (7) is determined by the relative magnitudes of the first two terms in the right hand side of the equation, which can then be calculated approximately by Eqs. (8) and (9).

There are two ideal situations in which the sign of the left hand side of Eq. (7) can be determined. First, when the signs of Eqs. (8) and (9) are positive, a net positive upward contravariant vertical wind is generated ($\dot{\xi}_{incorrect} - \dot{\xi} > 0$). This can occur at grid cells which are located southwest of a high perturbation pressure center with southwest wind ($\frac{\partial p'}{\partial \hat{x}^1} > 0, u > 0$; $\frac{\partial p'}{\partial \hat{x}^2} > 0, v > 0$). Second, when the signs of both Eqs. (8) and (9) are negative, a net negative downward contravariant vertical wind is produced ($\dot{\xi}_{incorrect} - \dot{\xi} < 0$). This can occur at grid cells which are located at the northeast of a low perturbation pressure center with northeast wind ($\frac{\partial p'}{\partial \hat{x}^1} > 0, u < 0$; $\frac{\partial p'}{\partial \hat{x}^2} > 0, v < 0$).

When the signs of Eqs. (8) and (9) are different, the sign of the left hand side of Eq. (7) has to be determined by the relative magnitude of Eqs. (8) and (9).

Since both the gradients of perturbation pressure and horizontal winds are weak for high perturbation pressure systems, the large differences of vertical wind velocities are much more pronounced in the low perturbation pressure centers than that in the high perturbation pressure centers

3. IMPACTS OF THE CORRECTION ON THE CONTRAVARIANT VERTICAL VELOCITIES GENERATED BY MCIP

3.1. Correlation of the vertical velocity error with weather pattern

To investigate the contravariant vertical wind velocity error and the impacts of the correction, the non-hydrostatic MM5 was run for a 42-km grid domain covering North America with 34 half-sigma levels for July 15-20 2002. MM5 output was processed with MCIPv3.2 (incorrect MCIP) and MCIPv3.3 (correct MCIP). The Jacobian and air density weighted contravariant vertical wind velocity (WHAT_JD) from MCIPv3.2 is referred to as the "incorrect vertical velocity" and that from MCIPv3.3 is referred to as the "correct vertical velocity". Both MCIPv3.2 and MCIPv3.3 collapsed the 34 layers in MM5 to 15 layers in MCIP.

As an example, Fig. 1(a) shows the surface perturbation pressure at 00UTC July 16, which is the beginning of the MCIP calculation, and the horizontal wind vector at 06UTC, July 16, 2002, and Fig. 1(b) shows the difference between the incorrect and correct WHAT_JD (incorrect minus correct values) at 06UTC, July 16. There are high correlations between the locations of the low perturbation pressure centers with strong western winds and those grid cells where there are large differences of vertical wind velocities. One deep low perturbation pressure center with large vertical wind difference can be seen over the northwestern Atlantic Ocean. The scattered small scale low perturbation pressure centers caused by high elevation terrains in the southwest of the domain also generate large differences of WHAT_JD.

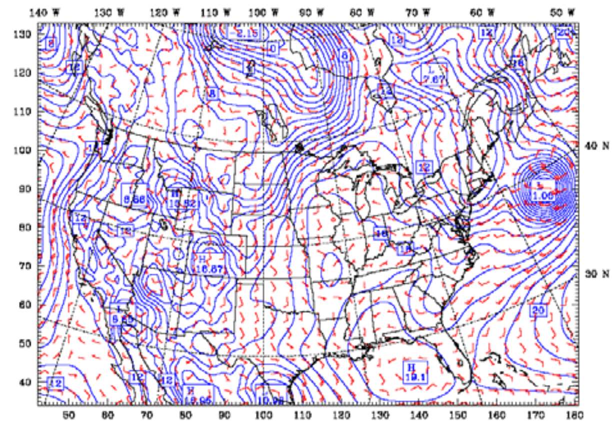

(a)

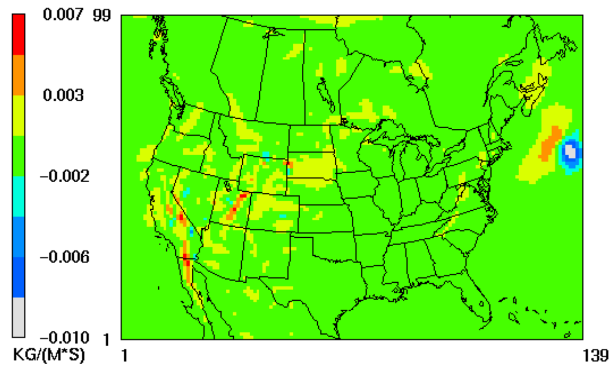

(b)

Fig. 1(a). Surface perturbation pressure at 00UTC, July, 16, and horizontal wind velocity vector at 06UTC, July 16 **(b)**. difference of Jacobian and air density weighted contravariant vertical velocity (incorrect minus correct values) at for 06UTC, July, 16.

3.2 Impact of the correction on the vertical velocity when surface front passes

A weak surface front passes southern Ontario around 18UTC (2pm EST), July 18 and terminates a three-day ozone pollution episode. Fig. 2(a) shows the hourly WHAT_JD values for the two cases, and their difference (incorrect minus correct) in the grid cell (99, 56), which is centered near Hamilton in southern Ontario. Fig. 2(b) shows the perturbation pressure at the first time step of the MCIP run and surface horizontal wind fields at 18UTC (2pm EST), July 18, 2002 for the southern Ontario areas. The upward vertical velocity is weakest at 07UTC (3am EST), but regains its peak value at 14UTC (10am EST). It weakens again quickly after 18UTC (2pm EST) when the front passes with intrusion of cold air (Fig. 2(a)).

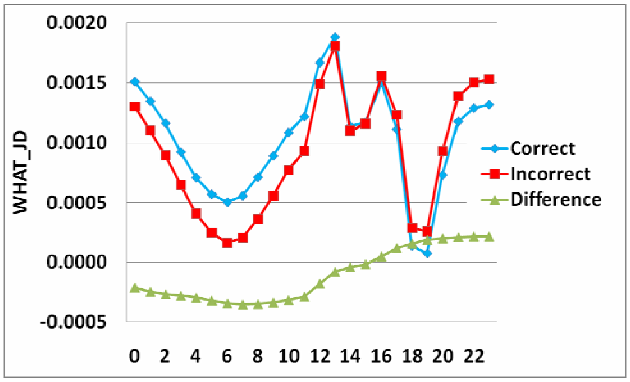

(a)

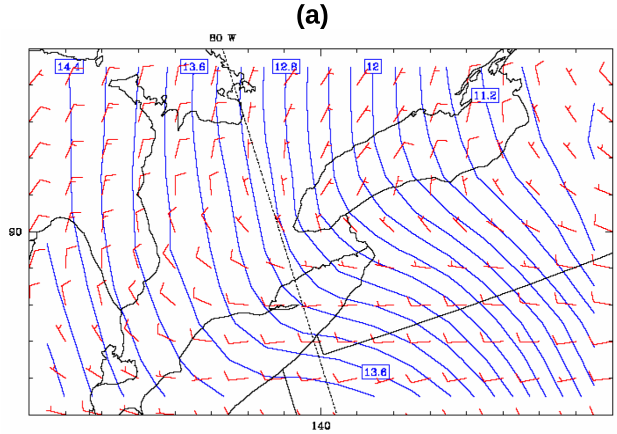

(b)

Fig. 2. (a) Hourly time series of the vertical wind velocity for July 18, 2002 for grid (99,56), which is centered with Hamilton, Southern Ontario; **(b).** Surface horizontal wind vector at 2pm EST (18UTC), July 18, 2002 and perturbation pressure for 00UTC, 16, July, 2002 in the same grid cell

Before the fontal pass, there is a negative difference in the vertical velocity because $\frac{\partial p'}{\partial \hat{x}^1} < 0, u > 0$, $\frac{\partial p'}{\partial \hat{x}^2} \cong 0, v \cong 0$ (Fig. 2(b)). The correct MCIP gave larger vertical wind velocities than the incorrect version. During the frontal passage, the vertical velocity difference diminishes because $\frac{\partial p'}{\partial \hat{x}^1} < 0, u \cong 0$ and $\frac{\partial p'}{\partial \hat{x}^2} \cong 0, v < 0$. The difference gradually shifts to positive after the front passed because $\frac{\partial p'}{\partial \hat{x}^1} < 0, u < 0$, $\frac{\partial p'}{\partial \hat{x}^2} \cong 0, v > 0$.

4. IMPACTS OF THE CORRECTION ON CMAQ RESULTS

4.1. Impact on air density advection results

Air density is advected at each time step and its ratio to the interpolated air density is used to calibrate the mixing ratio of other species at each step.

After 24 hours of advection, the incorrect vertical wind velocity produces unphysical air density with the domain maximum 6.9kg/m^3 and minimum 0.06kg/m^3. In contrast, the correct vertical wind velocity produces more reasonable air density, with the domain maximum 1.3 kg/m^3 and minimum 0.44 kg/m^3 (not shown).

4.2. Impact on Mass Consistency Adjustment

Hourly outputs from both the incorrect and correct MCIP are used in CMAQ to quantify the impact of the correction on mass consistency adjustments required by the Parabolic Piecewise Method (PPM) advection scheme used in CMAQ.

CMAQ employs two mass adjustment approaches. The default "YAMO" approach recalculates the vertical wind field with MCIP horizontal contravariant wind components. The MCIP error reported here does not affect the advection results using this method.

The "DENRATE" approach in CMAQ corrects concentration fields based on the ratio of advected and interpolated air density, called mass-adjustment ratio, at each advection time step. The error in MCIP vertical contravariant velocity significantly alters the mass consistency adjustment ratio due to incorrect transport of the air density 'tracer'.

Fig. 3(a) and Fig. 3(b) show the spatial distribution of the mass-adjustment ratio calculated with the incorrect and correct MCIP, respectively, after a 24 hour simulation. The air density tracer is advected over 24 hours rather than being updated at every advection time step. Significant differences are observed both spatially and in magnitude. Using the incorrect MCIP, the adjustment ratio is more chaotic with magnitude ranging from 0.17 to 22. In contrast, the correct MCIP gives the ratio ranging from 0.76 to 2.5, with few cells exceeding 1.5. The grid cells with high ratios are mostly at the high elevation terrain areas.

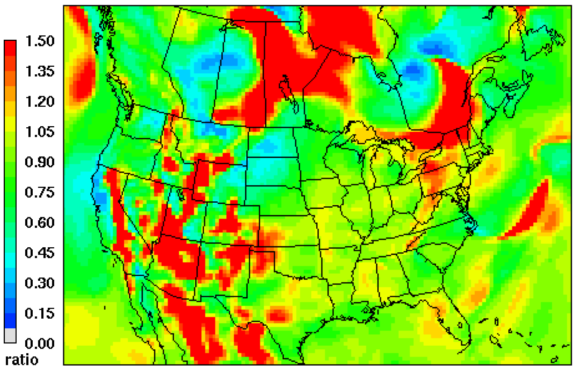

(a)

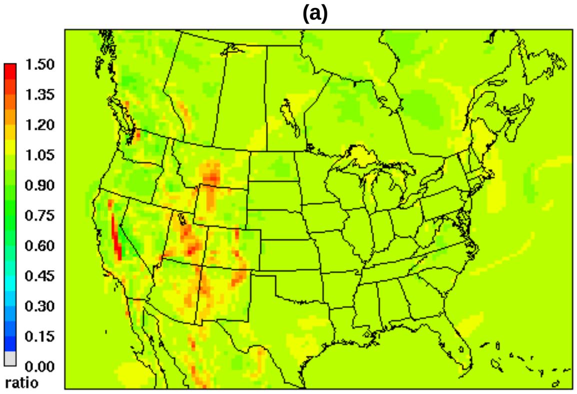

(b)

Fig. 3. Mass adjustment ratios after 24-hour advection with **(a)** the incorrect MCIP and **(b)** the correct MCIP simulation. Note the great differences in Northeast USA and Southern Ontario, Canada; in the provinces of Manitoba and Ontario and some grid cells on open sea.

Fig. 4 shows the hourly values of domain maximum and minimum mass-adjustment ratios generated by using the two MCIP versions for the first 24-hour period. The mass-adjustment ratios associated with the incorrect MCIP diverge and the adjustment required is an order of magnitude larger than that associated with the correct MCIP case. With the vertical velocity correction, the mass-adjustment ratios are generally in the range of 0.75 and 2.5, which is much closer to unity than that without the correction.

The results demonstrate that the mass inconsistency errors in the CMAQ advection scheme using the non-hydrostatic MM5 wind field and air density are not as serious as perceptions based on some previous studies e.g., (Lee, 2004)
.

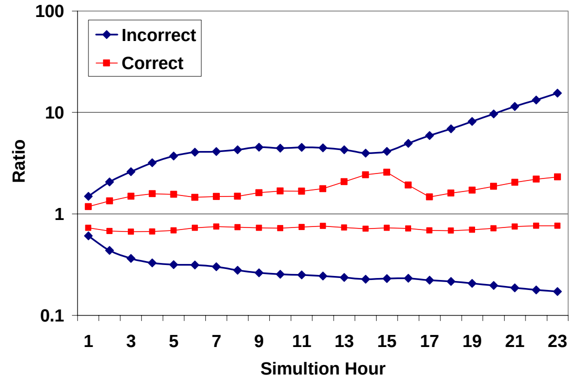

Fig. 4. Hourly time series of the domain maximum and minimum mass-adjustment ratio for correct and incorrect MCIP simulations.

4.3. Impact on Tracer Concentrations

A tracer with unit concentration (1 ppmv) was incorporated in a CMAQ simulation with advection process only. There was no mass adjustment to correct the mass inconsistency caused by the advection. Deviations from the unit concentration would indicate the extent of the mass-inconsistency caused by CMAQ advection.

The advection results after 24 hours show that the mass consistency error associated with the incorrect MCIP is sporadic, resulting in domain maximum concentration of 4.4 ppmv (Fig. 5(a)). In contrast, the domain maximum concentration is only 1.4 ppmv when the the correct MCIP results are used in the simulation, and most grid cells with large errors are in the high elevation terrain areas (Fig. 5(b)).

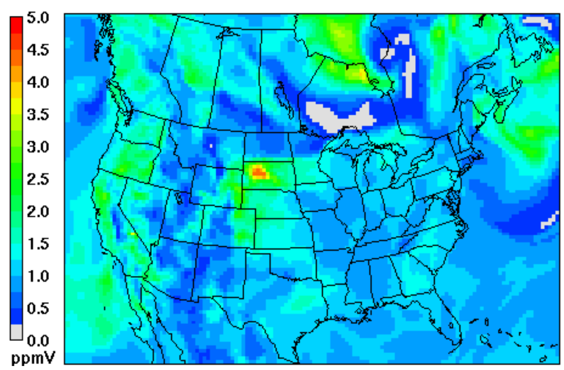

(a)

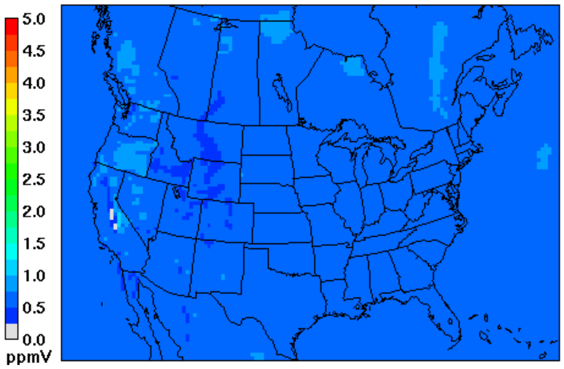

(b)

Fig. 5. Tracer concentrations after 24-hour advection when **(a)** the incorrect and **(b)** the correct MCIP results are used in the simulation.

5. CONCLUSION AND DISCUSSION

The mass inconsistency problem associated with using non-hydrostatic MM5 and MCIP results is not as serious as it has been previously regarded. The problem is partly caused by a mistake in calculating the contravariant vertical wind velocity in MCIP. This error caused incorrect tracer advection and exaggerated the mass inconsistency ratios associated with the non-hydrostatic MM5 results. The error has now been corrected in MCIP3.3.

Although the sigma formulation in non-hydrostatic MM5 allow the propagation of its individual terrain features upward to all sigma levels, even to the model top, this study shows that the mass adjustment ratios at the middle layers of CMAQ simulations are very close to unity (see Fig. 6). When developing new advection schemes, this consistency between air density and wind fields in the middle layers need to be carefully maintained and should not be disturbed without sound physical basis. Efforts should be spent to avoid propagating the errors at the lowest sigma layers upward, which would destroy the good mass consistency at the middle layers.

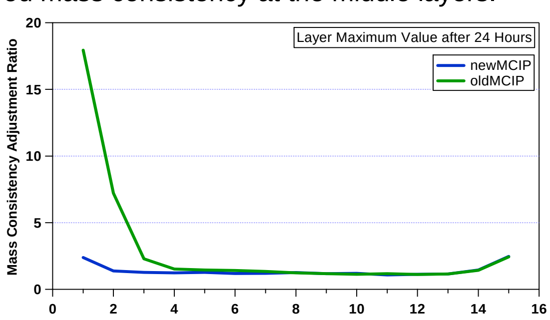

Fig. 6. Domain maximum mass adjustment ratios at the model vertical half sigma layers

6. REFERENCES

Anthes, R.A. and T.T. Warner, 1978: Development of hydrodynamic models suitable for air pollution and other mesometeorological studies. *Mon. Wea. Rev.,* 106, 1045-1078.

Byun, D. W., 1999a: Dynamically consistent formulations in meteorological and air quality models for multiscale atmospheric studies. Part I. Governing equations in a generalized coordinate system. *J. Atmos. Sci.,* **56**, 3789-3807.

Byun, D. W., 1999b: Dynamically consistent formulations in meteorological and air quality, models for multiscale atmospheric studies. Part II: Mass conservations issues. *J. Atmos Sci.,* **56**, 3808-3820.

Byun, D.W., and Ching, J.K.S., 1999: Science algorithms of the EPA Models-3 Community Multiscale Air Quality (CMAQ) Modeling System, U.S. EPA/600/R-99/030.

Dudhia, J., 1993: A nonhydrostatic version of the Penn State–NCAR, Mesoscale Model: Validation tests. *Mon. Wea. Rev.,* **121,** 1493–1513.

Dudhia J., Dave Gill, Kevin Manning, and Wei Wang, 2005: PSU/NCAR Mesoscale Modeling System Tutorial Class Notes and User's Guide: *MM5 Modeling System, Version 3*

Grell, G.A., J. Dudhia, and D.R. Stauffer, 1994: A Description of the Fifth-Generation PENN STATE/NCAR Mesoscale Model (MM5), NCAR Technical Note, NCAR/TN-398+*STR*

Kitada, T., 1987: Effect of non-zero divergence wind fields on atmospheric transport calculations. *Atmos. Environ.,* **21,** 785–788

Klaus P. Hoinka and Günther Zängl., 2004: The influence of the Vertical Coordinate on Simulations of a PV Streamer Crossing the Alps; *Mon Wea Rev*, 1860–1867

Lee, S.M., Yoon, S.C., and Byun D.W., 2004: The effect of mass inconsistency of the meteorological field generated by a common meteorological model on air quality modeling. *Atmos. Environ*. ,38, 2917-2926.

Murry L. Salby, 1996: Atmospheric physics, p166-194

Pielke, R. A., 2002: *Mesoscale Meteorological Modeling.* Academic Press, p122-160

Yin, D., 2004: A Description of the Extension for Using Canadian GEM data in MCIP and a Brief User's Guide for GEM-MCIP. ICPET, National Research Council of Canada.